
Learning Correlated Latent Representations with Adaptive Priors

Da Tang

Columbia University
datang@cs.columbia.edu

Dawen Liang

Netflix Inc.
dliang@netflix.com

Nicholas Ruozzi

The University of Texas at Dallas
nicholas.ruozzi@utdallas.edu

Tony Jebara

Columbia University & Netflix Inc.
jebara@cs.columbia.edu

Abstract

Variational Auto-Encoders (VAEs) have been widely applied for learning compact low-dimensional latent representations for high-dimensional data. When the correlation structure among data points is available, previous work proposed Correlated Variational Auto-Encoders (CVAEs) which employ a structured mixture model as prior and a structured variational posterior for each mixture component to enforce the learned latent representations to follow the same correlation structure. However, as we demonstrate in this paper, such a choice can not guarantee that CVAEs can capture all of the correlations. Furthermore, it prevents us from obtaining a tractable joint and marginal variational distribution. To address these issues, we propose Adaptive Correlated Variational Auto-Encoders (ACVAEs), which apply an adaptive prior distribution that can be adjusted during training, and learn a tractable joint distribution via a saddle-point optimization procedure. Its tractable form also enables further refinement with belief propagation. Experimental results on two real datasets show that ACVAEs outperform other benchmarks significantly.

1 Introduction

Variational Auto-Encoders (VAEs) [13, 22] are a family of deep generative models that learn latent embeddings for data. By applying variational inference on the latent variables, VAEs learn a stochastic mapping from high-dimensional data to low-dimensional representations, which can be used for many downstream tasks, including classification, regression, and clustering.

VAEs assume the data points are *i.i.d.* generated and treat the model and posterior approximations as factorized over data points. However, if we know *a priori* that there is structured correlation between the data points, e.g., for graph-structured datasets [23, 3, 8, 26], correlated variational approximations can help. Tang et al. [26] proposed Correlated Variational Auto-Encoders (CVAEs), which take this kind of correlation structure as auxiliary information to guide the variational approximations for the latent embeddings by taking a prior as a uniform mixture of tractable distributions on *maximal acyclic subgraphs* of the given undirected correlation graph.

However, there are several limitations that potentially prevent CVAEs from learning better correlated latent embeddings. First, it is possible that some of the maximal acyclic subgraphs of the given graph can, by themselves, well-capture the correlation between the data points while others may poorly capture the correlation. As a result, taking a uniform average may yield a sub-optimal result. Second, while the prior CVAEs is over multiple subgraphs, each subgraph has a unique joint variational distribution, and there is no single *global* joint variational distribution over the latent variables. In

addition, CVAEs require a pre-processing step that takes an amount of time cubic in the number of vertices, which limits its applicability to smaller datasets.

To address these issues, we propose Adaptive Correlated Variational Auto-Encoders (ACVAEs), which chooses a non-uniform average over tractable distributions on the maximal acyclic subgraphs as a prior. This prior is adaptive, and will be adjusted during optimization. We apply a saddle-point optimization procedure that maximizes the objective with respect to the model and variational parameters and minimizes the objective with respect to the prior structure for more robust inference. The non-uniform average converges to a tractable prior on a single graph, which ensures that we obtain a holistic tractable joint variational distribution. With this variational distribution, we obtain more accurate marginal evaluation using exact inference algorithms (e.g., belief propagation). Moreover, Adaptive Correlated Variational Auto-Encoders do not require the cubic time pre-processing step embedded in CVAEs.

We demonstrate the superior empirical performance of Adaptive Correlated Variational Auto-Encoders for link prediction on various real datasets.

2 VAEs with correlations

In this section, we provide a brief overview of Variational Auto-Encoders (VAEs) [13, 22] as well as Correlated Variational Auto-Encoders (CVAEs) [26] which take the correlation structure among data points into consideration.

2.1 Variational Auto-Encoders

We use a latent variable model to fit data $\mathbf{x} = \{x_1, \dots, x_n\} \subset \mathbb{R}^D$. The model assumes that there exist low-dimensional latent embeddings for each data point $\mathbf{z} = \{z_1, \dots, z_n\} \subset \mathbb{R}^d$ ($d \ll D$), which come from a prior distribution $p_0(\cdot)$, and x_i 's are drawn conditionally independently given z_i . Denote the model parameters as θ . The likelihood of this model is $p_\theta(\mathbf{x}) = \prod_{i=1}^n \int p_0(z_i) p_\theta(x_i|z_i) dz_i$.

To simultaneously learn the model parameter θ as well as a mapping from the observed data \mathbf{x} to the latent embeddings \mathbf{z} , Variational Auto-Encoders (VAEs) [13, 22] apply a data-dependent variational approximation $q_\lambda(\mathbf{z}|\mathbf{x}) = \prod_{i=1}^n q_\lambda(z_i|x_i)$, where λ denotes the variational parameters, and maximize the *evidence lower-bound* (ELBO) on the log-likelihood of the data, $\log p_\theta(\mathbf{x})$:

$$L(\lambda, \theta) = \mathbb{E}_{q_\lambda(\mathbf{z}|\mathbf{x})} [\log p_\theta(\mathbf{x}|\mathbf{z})] - \text{KL}(q_\lambda(\mathbf{z}|\mathbf{x}) || p_0(\mathbf{z})). \quad (1)$$

2.2 Correlated Variational Auto-Encoders

Standard VAEs are capable of learning compact low-dimensional embeddings for high-dimensional data. However, due to the i.i.d. assumption, they fail to account for the correlations between data points when *a priori* we know correlations exist. Correlated Variational Auto-Encoders (CVAEs) [26] mitigate the issue by employing a structured prior as well as a structured variational posterior to take advantage of the structured correlation information.

Formally, assume we are given an undirected correlation graph $G = (V, E)$, where $(v_i, v_j) \in E$ represents that the data points x_i and x_j are correlated, CVAEs apply a correlated prior $p_0^{\text{corr}}(\mathbf{z})$ on the latent variables \mathbf{z}_i 's which satisfies

$$p_0^{\text{corr}}(z_i) = p_0(z_i) \text{ for all } v_i \in V, \quad p_0^{\text{corr}}(z_i, z_j) = p_0(z_i, z_j) \text{ if } (v_i, v_j) \in E. \quad (2)$$

Here $p_0(\cdot)$ and $p_0(\cdot, \cdot)$ are parameter-free functions that capture the singleton and pairwise marginal distributions of the latent variables. For example, we can set $p_0(\cdot)$ to be the density of a standard multivariate normal distribution and $p_0(\cdot, \cdot)$ to be a multivariate normal density that has high values if the two inputs are close to each other. With such a prior, we again assume x_i 's are drawn conditionally independently given z_i . When G is acyclic, such a prior $p_0^{\text{corr}}(\mathbf{z})$ does exist [28]:

$$p_0^{\text{corr}}(\mathbf{z}) = \prod_{i=1}^n p_0(z_i) \prod_{(v_i, v_j) \in E} \frac{p_0(z_i, z_j)}{p_0(z_i)p_0(z_j)}. \quad (3)$$

However, when G is not acyclic, Eq. 3 is not necessarily a valid probability density function. To deal with this issue, CVAEs propose constructing a prior that is a mixture over the set \mathcal{A}_G of all of G 's *maximal acyclic subgraphs*, which are defined as follows:

Definition 1 (Maximal acyclic subgraph). *For an undirected graph $G = (V, E)$, an acyclic subgraph $G' = (V', E')$ is a maximal acyclic subgraph of G if:*

- $V' = V$, i.e., G' contains all vertices of G .
- Adding any edge from E/E' to E' will create a cycle in G' .

Each of the maximal acyclic subgraphs $G' \in \mathcal{A}_G$ can partially approximate the correlation structure in G , and CVAEs set the prior $p_0^{\text{corr}_g}(\mathbf{z})$ to be the uniform average over all of these tractable densities:

$$p_0^{\text{corr}_g}(\mathbf{z}) = \frac{1}{|\mathcal{A}_G|} \sum_{G'=(V,E') \in \mathcal{A}_G} p_0^{G'}(\mathbf{z}), \quad (4)$$

where $p_0^{G'}(\mathbf{z}) = \prod_{i=1}^n p_0(\mathbf{z}_i) \prod_{(v_i, v_j) \in E'} \frac{p_0(\mathbf{z}_i, \mathbf{z}_j)}{p_0(\mathbf{z}_i)p_0(\mathbf{z}_j)}$ is a prior on a maximal acyclic subgraph $G' = (V, E')$ with the same form as in Eq. 3. For each $G' \in \mathcal{A}_G$, we can similarly define a structured variational approximation $q_{\lambda}^{G'}(\mathbf{z}|\mathbf{x})$ following the form of Eq. 3 (see appendix for details). With this structured prior as well as variational posterior, CVAEs optimize a different form of ELBO:

$$\begin{aligned} \log p_{\theta}(\mathbf{x}) &= \mathbb{E}_{p_0^{\text{corr}_g}(\mathbf{z})} [\log p_{\theta}(\mathbf{x}|\mathbf{z})] = \frac{1}{|\mathcal{A}_G|} \sum_{G' \in \mathcal{A}_G} \mathbb{E}_{p_0^{G'}(\mathbf{z})} [\log p_{\theta}(\mathbf{x}|\mathbf{z})] \\ &\geq \frac{1}{|\mathcal{A}_G|} \sum_{G' \in \mathcal{A}_G} \left(\mathbb{E}_{q_{\lambda}^{G'}(\mathbf{z}|\mathbf{x})} [\log p_{\theta}(\mathbf{x}|\mathbf{z})] - \text{KL}(q_{\lambda}^{G'}(\mathbf{z}|\mathbf{x}) || p_0^{G'}(\mathbf{z})) \right). \end{aligned} \quad (5)$$

Even though empirically Tang et al. [26] show that CVAEs are capable of capitalizing on the correlation structure as auxiliary information when learning latent embeddings, there are a few limitations to this approach. First of all, the ELBO in Eq. 5 is defined as a uniform average over individual ELBOs for all of the maximal acyclic subgraph $G' \in \mathcal{A}_G$, and each G' posits a different variational approximation $q_{\lambda}^{G'}(\mathbf{z}|\mathbf{x})$. As a result, we can not obtain a holistic variational distribution $q_{\lambda}(\mathbf{z}|\mathbf{x})$ as the approximation to the posterior distribution $p(\mathbf{z}|\mathbf{x})$. Moreover, not every maximal acyclic subgraph is capable of capturing the correlation well, hence taking a uniform average over all of them can be sub-optimal. Last but not least, from a computational standpoint, to mitigate the intractable average over \mathcal{A}_G which can contain exponentially many elements, the algorithm proposed in Tang et al. [26] requires a $O(|V|^3)$ pre-processing step. This prevents the algorithm from being applied to large-scale datasets. In the next section, we will propose fixes to all of these limitations.

3 Adaptive Correlated VAEs

3.1 A non-uniform mixture prior

As motivated in Section 2.2, rather than using a uniform average, we instead employ a categorical distribution $\pi \in \Delta^{|\mathcal{A}_G|-1}$ representing the normalized weights over all maximal acyclic subgraphs $G' \in \mathcal{A}_G$ of G . Recall the ELBO in Eq. 5, we can replace the uniform average in the prior $p_0^{\text{corr}_g}(\mathbf{z})$ in Eq. 4 with the non-uniform distribution π , which gives us the following ELBO:

$$\begin{aligned} &\mathbb{E}_{G' \sim \pi} \left[\mathbb{E}_{q_{\lambda}^{G'}(\mathbf{z}|\mathbf{x})} [\log p_{\theta}(\mathbf{x}|\mathbf{z})] - \text{KL}(q_{\lambda}^{G'}(\mathbf{z}|\mathbf{x}) || p_0^{G'}(\mathbf{z})) \right] \\ &\leq \mathbb{E}_{G' \sim \pi} \left[\mathbb{E}_{p_0^{G'}(\mathbf{z})} [\log p_{\theta}(\mathbf{x}|\mathbf{z})] \right] := \mathbb{E}_{p_0^{\pi}(\mathbf{z})} [\log p_{\theta}(\mathbf{x}|\mathbf{z})] = \log p_{\pi, \theta}(\mathbf{x}). \end{aligned} \quad (6)$$

Here we define the non-uniform prior $p_0^{\pi}(\mathbf{z}) = \mathbb{E}_{G' \sim \pi} [p_0^{G'}(\mathbf{z})]$. From the above inequality we can see that, using the non-uniform prior p_0^{π} , we are still able to obtain a lower bound of the log-likelihood $\log p_{\pi, \theta}(\mathbf{x})$, which is now also parametrized by the weight parameter π . If we optimize this categorical distribution π together with all the other parameters, the above loss function implies that we are optimizing with an adaptive prior. Hence, we call the above model Adaptive Correlated

Variational Auto-Encoders (ACVAEs). If we replace π with a uniform distribution over all subgraphs in \mathcal{A}_G , we recover CVAEs.

Plugging $q_{\lambda}^{G'}(z|\mathbf{x})$ and $p_0^{G'}(z)$ from Section 2.2 into Eq. 6, yields the following ELBO for ACVAEs:

$$\begin{aligned} \mathcal{L}^{\text{ACVAE}}(\pi, \lambda, \theta) := & \sum_{i=1}^n \left(\mathbb{E}_{q_{\lambda}(z_i|\mathbf{x}_i)} [\log p_{\theta}(\mathbf{x}_i|z_i)] - \text{KL}(q_{\lambda}(z_i|\mathbf{x}_i)||p_0(z_i)) \right) - \sum_{(v_i, v_j) \in E} w_{G, \pi, (v_i, v_j)}^{\text{MAS}} \\ & \cdot \left(\text{KL}(q_{\lambda}(z_i, z_j|\mathbf{x}_i, \mathbf{x}_j)||p_0(z_i, z_j)) - \text{KL}(q_{\lambda}(z_i|\mathbf{x}_i)||p_0(z_i)) - \text{KL}(q_{\lambda}(z_j|\mathbf{x}_j)||p_0(z_j)) \right). \end{aligned} \quad (7)$$

Similar to CVAEs, we have edge weights $w_{G, \pi, (v_i, v_j)}^{\text{MAS}}$ representing the expected appearance probability for edge (v_i, v_j) over the set of maximal acyclic subgraphs \mathcal{A}_G given the distribution π . In the following definition, we abusively write $\pi(G')$ as the probability of G' being sampled from \mathcal{A}_G .

Definition 2 (Non-uniform maximal acyclic subgraph edge weight). *For an undirected graph $G = (V, E)$, an edge $e \in E$ and a distribution π on the set \mathcal{A}_G of maximal acyclic subgraphs of G , define $w_{G, \pi, e}^{\text{MAS}}$ to be the expected appearance probability of the edge e in a random maximal acyclic subgraph $G' = (V, E') \sim \pi$, i.e., $w_{G, \pi, e}^{\text{MAS}} := \sum_{G' \in \mathcal{A}_G, e \in E'} \pi(G')$.*

3.2 A minimax objective

With the loss function in Eq. 7, an intuitive direction would be to perform empirical Bayes [7] and directly maximize $\mathcal{L}^{\text{ACVAE}}(\pi, \lambda, \theta)$ with respect to all the parameters π , λ and θ . An important observation is that for fixed λ and θ , the loss function $\mathcal{L}^{\text{ACVAE}}$ is linear w.r.t. the weight parameter π . Therefore, if optima for $\mathcal{L}^{\text{ACVAE}}(\pi, \lambda, \theta)$ exist, then at least one optimum will have a π^* which puts all of its probability mass on a single subgraph G'^* . This optimum drastically simplifies the structured prior p_0^{π} . However, empirically we observe that it often fails to generalize the learned correlations well.

On the other hand, we can achieve more robust inference by considering a minimax saddle-point optimization:

$$\max_{\lambda, \theta} \min_{\pi} \mathcal{L}^{\text{ACVAE}}(\pi, \lambda, \theta). \quad (8)$$

As the optimization objective indicates, we are optimizing the ELBO under the prior that produces the *lowest* lower bound. The intuition is that if we can even optimize the worst lower bound well, the variational distribution and the model distribution we learn would be robust and generalize better. This is similar to the *least favorable prior*, under which a Bayes estimator can achieve minimax risk [14]. In Section 5, we show the effectiveness of this saddle-point optimization, compared to the empirical Bayes procedure.

Proposition 1 (Optimum for π). *If the saddle-point optimization in Eq. 8 has global optima, then at least one optimum $(\pi^*, \lambda^*, \theta^*)$ will have a π^* that places all of its probability mass on a single maximal acyclic subgraph $G'^* \in \mathcal{A}_G$.*

By this proposition, we know that the optimization in Eq. 8 will return us a single subgraph G'^* , similar to empirical Bayes. At this optimum, the loss function becomes the ELBO on a single acyclic subgraph G'^* , with $q_{\lambda^*}^{G'^*}(z|\mathbf{x})$ as the variational distribution. Therefore, we have a holistic variational approximation, overcoming one of the limitations of CVAEs. We will show in Section 3.4 that we can further refine the variational approximation by making use of the single-acyclic-subgraph structure for $q_{\lambda^*}^{G'^*}(z|\mathbf{x})$.

3.3 Learning with alternating updates

Direct optimization of the saddle-point problem is non-trivial. Following similar saddle-point optimization for a spanning tree structured upper bound for the log-partition function of undirected graphical models [29, 30], we perform an alternating optimization on the parameters λ , θ and π . Details are shown in Algorithm 1.

Updates for π When the variational parameter λ and the model parameter θ are fixed, the loss function $\mathcal{L}^{\text{ACVAE}}(\pi, \lambda, \theta)$ is linear in π . However, we cannot directly optimize over $\pi \in \Delta^{|\mathcal{A}_G|-1}$, as

Algorithm 1 ACVAEs learning

Input: data $\mathbf{x}_1, \dots, \mathbf{x}_n \in \mathbb{R}^D$, undirected graph $G = (V = \{v_1, \dots, v_n\}, E)$, parameter $\gamma > 0$.
Initialize the parameters λ, θ . Initialize the weights $w_{G,\pi,e}^{\text{MAS}^{t+1}}$ for each $e \in E$.
while not converged **do**
 Optimize the parameters (λ, θ) using the gradients $\nabla_{\lambda,\theta} \mathcal{L}^{\text{ACVAE}}(\pi, \lambda, \theta)$.
 Compute the mass $m_{(v_i, v_j)}$ for each edge $e \in E$ with Eq. 9.
 Compute a minimum spanning tree of the graph with the masses $m_{(v_i, v_j)}$'s as the edge weights
 and update the weights $w_{G,\pi,e}^{\text{MAS}}$ for each $e \in E$ according to Eq. 10.
end while
Return: The parameters λ, θ , the weights $w_{G,\pi,e}^{\text{MAS}}$ for each $e \in E$.

it may contain exponentially many dimensions. We can instead update the edge weights $w_{G,\pi,(v_i, v_j)}^{\text{MAS}}$ as the loss function is also linear in the edge weights.

By definition, we know that each maximal acyclic subgraph G' of G is a forest, consisting of one spanning tree for each connected component of G . Therefore, the domain for the edge weights $\bigcup_{e \in E} \{w_{G,\pi,e}^{\text{MAS}}\}$ is the projection of the Cartesian product of the spanning tree polytopes for all connected components of G [29, 30] to the edge weight space. This Cartesian product on the polytopes is convex and its boundary is determined by potentially exponentially many linear inequalities. Despite that, directly optimizing $\mathcal{L}^{\text{ACVAE}}(\pi, \lambda, \theta)$ with respect to these weights $\bigcup_{e \in E} \{w_{G,\pi,e}^{\text{MAS}}\}$ is in fact tractable:

the optimum for $\min_{\pi} \mathcal{L}^{\text{ACVAE}}(\pi, \lambda, \theta)$ is obtained at $\hat{\pi}$ that has all the mass on a single maximal acyclic subgraph \hat{G}' . This means the optimum for these edges weights can be obtained from a single subgraph \hat{G}' . By re-arranging terms in Eq. 7 with respect to $\bigcup_{e \in E} \{w_{G,\pi,e}^{\text{MAS}}\}$, it is not difficult to see

that \hat{G}' should have the smallest “edge mass” sum over all maximal acyclic subgraphs \mathcal{A}_G , where the “edge mass” $m_{(v_i, v_j)}$ of edge $e = (v_i, v_j)$ is:

$$m_{(v_i, v_j)} := \text{KL}(q_{\lambda}(z_i, z_j | \mathbf{x}_i, \mathbf{x}_j) || p_0(z_i, z_j)) - \text{KL}(q_{\lambda}(z_i | \mathbf{x}_i) || p_0(z_i)) - \text{KL}(q_{\lambda}(z_j | \mathbf{x}_j) || p_0(z_j)), \quad (9)$$

which means \hat{G}' is the combination of the minimum spanning trees of all connected components of the graph with $m_{(v_i, v_j)}$ as the weights.

Once we identify \hat{G}' , the optimal weights $\hat{w}_{G,\pi,e}^{\text{MAS}}$ are either 1 (if the edge e is selected) or 0 (otherwise). Instead of directly updating the weights to the optimal values, we perform a soft update with step size α^t at iteration t , similar to Wainwright [29], Wainwright et al. [30]:

$$w_{G,\pi,e}^{\text{MAS}^{t+1}} \leftarrow (1 - \alpha^t) w_{G,\pi,e}^{\text{MAS}^t} + \alpha^t \hat{w}_{G,\pi,e}^{\text{MAS}}. \quad (10)$$

This soft update helps prevent the algorithm from becoming trapped in bad local optima early in the optimization procedure. The step size α^t can be either a constant or dynamically adjusted during optimization. We set it to be a constant in our experiments.

One of the limitations of CVAEs mentioned in Section 2.2 is the $O(|V|^3)$ pre-processing step to compute all the edge weights $w_{G,e}^{\text{MAS}}$. We alleviate this bottleneck in ACVAEs, as it only takes $O(\min(|V|^2, |E| \log |V|))$ operations per initialization to update on the weights, which ensures that ACVAEs can scale to datasets with many more vertices than would be feasible with CVAEs.

Updates for λ and θ When π is fixed, λ and θ can be updated by taking a stochastic gradient step following $\nabla_{\lambda,\theta} \mathcal{L}^{\text{ACVAE}}(\pi, \lambda, \theta)$ with reparametrization gradient [13, 22], as done in standard VAEs.

It is difficult to make any general statement about the convergence of Algorithm 1 as they perform a saddle-point optimization with non-convex objective. Empirically we find that Algorithm 1 is stable and performs well on multiple real datasets.

3.4 Refine posterior approximation with belief propagation

From Proposition 1, we know the weights $w_{G,\pi,e}^{\text{MAS}}$ returned from Algorithm 1 are from a single maximal acyclic subgraph $G' \in \mathcal{A}_G$. Consequently, we have a holistic variational approximation

$q_{\lambda}^{G'}(z|x)$. The acyclic structure of G' makes it possible to further refine the pairwise marginal approximation between any pair of vertices via a belief-propagation-style [20] message-passing algorithm, which is not possible for CVAEs, as it does not have a single joint variational distribution on z . This can be crucial in tasks in which we need an accurate pairwise marginal approximation, e.g., link prediction.

Consider any $v_i \neq v_j \in V$ that are in the same connected component of G' . Since G' is acyclic there is a unique path from v_i to v_j . Denote it as $v_i = u_0^{i,j} \rightarrow u_1^{i,j} \rightarrow \dots \rightarrow u_{k_{i,j}}^{i,j} = v_j$. The refined pairwise marginal $r_{\lambda}(z_i, z_j | x_i, x_j)$ is defined to be:

$$r_{\lambda}(z_i, z_j | x_i, x_j) = \int \prod_{l=0}^{k_{i,j}-1} q_{\lambda}(z_{u_l^{i,j}}, z_{u_{l+1}^{i,j}} | x_{u_l^{i,j}}, x_{u_{l+1}^{i,j}}) \prod_{l=1}^{k_{i,j}-1} \frac{dz_{u_l^{i,j}}}{q_{\lambda}(z_{u_l^{i,j}} | x_{u_l^{i,j}})}. \quad (11)$$

The above pairwise marginal densities can be computed for all pairs of (v_i, v_j) by doing a depth-first search or a breadth-first search starting from each $v_i \in V$ after we obtain the variational approximation $q_{\lambda}^{G'}(z|x)$ from Algorithm 1, which has a total complexity of $O(|V|^2)$, the same as evaluating every pairwise marginal in CVAEs. For the remainder of the paper, unless otherwise specified, we always apply the belief propagation refinement to ACVAEs. As we show in Section 5, this refinement with belief propagation dramatically improves the quality of the pairwise marginal approximation.

4 Related Work

This work extends CVAEs with the idea of learning a non-uniform average loss over some tractable loss functions on maximal acyclic subgraphs of the given graph. This is similar to the idea of obtaining a tighter upper bound on the log-partition function for an undirected graphical model by minimizing over a convex combination of spanning trees of the given graph [30]. To optimize the parameters, Wainwright et al. [30] also apply alternating updates on the parameters and the distributions over the spanning trees, similar to the approach in ACVAE learning. Alternating parameter updates are useful for many other cases. For example, Alternating Least Squares for matrix factorization [24] and Alternating Direction Method of Multipliers (ADMM) for convex optimization [4, 25, 10].

Some recent work also focuses on incorporating correlation structures over latent variables. For example, Hoffman and Blei [9] proposed structured variational families that can improve over traditional mean-field variational inference. Johnson et al. [11] proposed Structured VAEs that apply more complex forms for the priors on the latent embeddings. Recently in the NLP community, Yin et al. [31] proposed utilizing tree-structured latent variable models to deal with semantic parsing. However, most of these work focuses on correlations *within* dimensions of latent variables whereas our work focus on correlations *between* latent variables, similar to the setting of CVAEs. In addition, Luo et al. [16] incorporated pairwise correlations between latent variables into deep generative models for semi-crowdsourced clustering.

In addition, another set of related work line in convolutional networks for graphs and their extensions [3, 6, 5, 19, 8, 27], which also take graph structure of data into considerations.

5 Experiment

In this section, we evaluate ACVAEs on the task of link prediction. We show that our method significantly outperforms various baselines. We perform careful corroboration to identify the contributing factor for the gain. Finally, we present a visualization of the learned correlated posterior variational approximation to illustrate the maximal acyclic subgraph \hat{G}' .

5.1 Experiment settings

5.1.1 Task

For the task of link prediction, we are given a correlation graph $G = (V = \{v_1, \dots, v_n\}, E)$ and a feature vector $x_i \in \mathbb{R}^N$ for each $i \in \{1, \dots, n\}$. Consistent with the setting of Tang et al. [26], we construct a heldout test set using $\max(1, \frac{\text{degree}(v_i)}{20})$ of the edges related to v_i , and use the remaining edges for training.

5.1.2 Datasets

We evaluate ACVAEs on the Epinions¹ [18], a public product rating dataset that contains $\approx 49\text{K}$ users and $\approx 140\text{K}$ products, and the High-energy physics theory citation network dataset² [15], a citation graph with $\approx 28\text{K}$ papers and $\approx 353\text{K}$ citation edges.

5.1.3 Baselines

We compare ACVAE with 4 baseline methods:

- VAE [13]: standard variational auto-encoders, with no information about the correlations.
- GraphSAGE [8]: the state-of-the-art method for learning latent embeddings that takes the correlation structure into account with graph convolutional neural networks.
- CVAE_{ind} and CVAE_{corr} [26]: Two variations of CVAEs with factorized and structured variational approximations, respectively.

5.1.4 Metrics

For all methods, we first learn latent embeddings z_1, \dots, z_n , which are deterministic for GraphSAGE and stochastic for the VAEs-related methods. Then we compute the pairwise distance $\text{dis}_{i,j}$ between each pair (z_i, z_j) of the latent embeddings. The distance $\text{dis}_{i,j}$ is defined as

$$\text{dis}_{i,j} = \begin{cases} \mathbb{E}_{r(z_i, z_j | x_i, x_j)} [\|z_i - z_j\|_2^2] & \text{for ACVAE} \\ \mathbb{E}_{q(z_i, z_j | x_i, x_j)} [\|z_i - z_j\|_2^2] & \text{for VAE and CVAE} \\ \|z_i - z_j\|_2^2 & \text{for GraphSAGE.} \end{cases}$$

For each user u_i , we compute the *Cumulative Reciprocal Rank* (CRR) as follows:

$$\text{CRR}_i = \sum_{(v_i, v_j) \in E_{\text{test}}} \frac{1}{|\{k : (v_i, v_k) \notin E_{\text{train}}, \text{dis}_{i,k} \leq \text{dis}_{i,j}\}|}.$$

A larger CRR value indicates the heldout edges have a higher rank among all the candidates. We further normalize the CRR values to be in $[0, 1]$, and report the normalized CRR (NCRR).

More details on data pre-processing and the experimental protocols can be found in the appendix.

5.2 Results

We show the heldout NCRR values in Table 1. ACVAE outperforms all the baseline methods by a wide margin. CVAEs outperform both VAEs and GraphSAGE in Tang et al. [26]. Therefore, we focus our attention to the comparison between CVAEs and ACVAEs. As motivated in Section 2.2, ACVAEs improve over the limitations of CVAEs by providing a holistic variational approximation as a result of the saddle-point optimization, which further enables applying belief propagation for more accurate marginal approximation. We look into each aspect individually.

Saddle-point optimization v.s. empirical Bayes From Section 3.2, we know that π will put all the probability mass on a single maximal acyclic graph in both the saddle-point optimization in Eq. 8 or empirical Bayes. We compare these two approaches on Epinions. For empirical Bayes, we observe a test NCRR of only 0.0300 ± 0.0093 , which is worse than ACVAEs with saddle-point optimization in Table 1(a). Interestingly, in Figure 1(a), we can see that empirical Bayes actually reaches much higher ELBOs, yet it fails to generalize as well as saddle-point optimization which proves more robust.

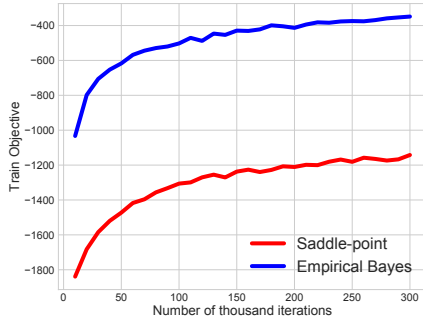
Belief propagation refinement We investigate the importance of using belief propagation refinement on Epinions: without it, we only observe a test NCRR of 0.0133 ± 0.0005 , a significant decline. This suggests that variational approximation can yield significantly different results when compared with exact inference (i.e., belief propagation) on an acyclic graph.

¹http://www.trustlet.org/downloaded_epinions.html

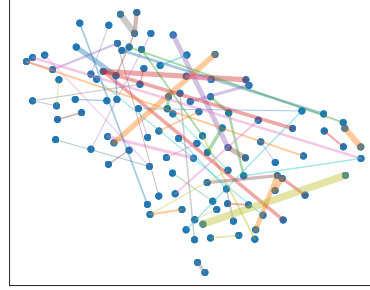
²<http://snap.stanford.edu/data/cit-HepTh.html>

Table 1: Link prediction normalized CRR

(a) Normalized CRR on Epinions		(b) Normalized CRR on Citations	
Name	Test NCRR	Name	Test NCRR
VAE	0.0052 ± 0.0007	VAE	0.0078 ± 0.0023
GraphSAGE	0.0115 ± 0.0025	GraphSAGE	0.0143 ± 0.0050
CVAE _{ind}	0.0160 ± 0.0004	CVAE _{ind}	0.0335 ± 0.0052
CVAE _{corr}	0.0171 ± 0.0009	CVAE _{corr}	0.0663 ± 0.0020
ACVAE	0.0434 ± 0.0014	ACVAE	0.1052 ± 0.0054



(a) Training learning curves for the Epinions experiment. Belief propagation evaluations are applied. We compare the training objective for saddle-point optimization and empirical Bayes optimization. It can be seen that the objective for empirical Bayes optimization is much better compared to that for the saddle-point optimization.



(b) Embeddings of an induced maximal acyclic subgraph \hat{G}' that ACVAEs learns on the citations experiment. The coordinates are t-SNE embeddings for the variational approximation mean of the latent variables. The edge widths represent the strength of the learned correlations. We can see some of the learned embeddings are not necessarily close to each other even when they have high correlations. Colors for better clarity only.

Figure 1: Training learning curves on Epinions and latent embedding visualization on Citations.

Figure 1(b) visualizes the largest connected component of the maximal acyclic subgraph $\hat{G}' = (V, \hat{E}')$ that ACVAE learns for the variational distribution on the citations dataset. We can see that, not all the vertices with edges in \hat{E}' are close to each other, which indicates that the learned \hat{G}' provides some additional information that singleton marginals cannot provide.

6 Conclusion

In this paper, we introduce ACVAEs, which learn a joint variational distribution on the latent embeddings of input data via saddle-point optimization of a loss function that is a non-uniform average over some tractable correlated ELBOs. The learned joint variational distribution can be used to perform efficient evaluations using belief propagation. Experiment results show that ACVAEs can outperform existing methods for link prediction on two real datasets. Future work will include learning higher-order correlations between latent variables.

References

- [1] Martín Abadi, Paul Barham, Jianmin Chen, Zhifeng Chen, Andy Davis, Jeffrey Dean, Matthieu Devin, Sanjay Ghemawat, Geoffrey Irving, Michael Isard, et al. Tensorflow: A system for large-scale machine learning. In *12th USENIX Symposium on Operating Systems Design and Implementation (OSDI 16)*, pages 265–283, 2016.

- [2] Stefan Behnel, Robert Bradshaw, Craig Citro, Lisandro Dalcin, Dag Sverre Seljebotn, and Kurt Smith. Cython: The best of both worlds. *Computing in Science & Engineering*, 13(2):31, 2011.
- [3] Joan Bruna, Wojciech Zaremba, Arthur Szlam, and Yann LeCun. Spectral networks and locally connected networks on graphs. In *3rd International Conference on Learning Representations*, 2015.
- [4] Antonin Chambolle and Thomas Pock. A first-order primal-dual algorithm for convex problems with applications to imaging. *Journal of mathematical imaging and vision*, 40(1):120–145, 2011.
- [5] Michaël Defferrard, Xavier Bresson, and Pierre Vandergheynst. Convolutional neural networks on graphs with fast localized spectral filtering. In *Advances in Neural Information Processing Systems*, pages 3844–3852, 2016.
- [6] David Duvenaud, Dougal Maclaurin, Jorge Iparraguirre, Rafael Bombarell, Timothy Hirzel, Alán Aspuru-Guzik, and Ryan Adams. Convolutional networks on graphs for learning molecular fingerprints. In *Advances in neural information processing systems*, pages 2224–2232, 2015.
- [7] Bradley Efron. *Large-scale inference: empirical Bayes methods for estimation, testing, and prediction*, volume 1. Cambridge University Press, 2012.
- [8] Will Hamilton, Zhitao Ying, and Jure Leskovec. Inductive representation learning on large graphs. In *Advances in Neural Information Processing Systems*, pages 1025–1035, 2017.
- [9] Matthew Hoffman and David Blei. Stochastic structured variational inference. In *Proceedings of the 18th International Conference on Artificial Intelligence and Statistics*, pages 361–369, 2015.
- [10] Mingyi Hong and Zhi-Quan Luo. On the linear convergence of the alternating direction method of multipliers. *Mathematical Programming*, 162(1-2):165–199, 2017.
- [11] Matthew Johnson, David Duvenaud, Alex Wiltchko, Ryan Adams, and Sandeep Datta. Composing graphical models with neural networks for structured representations and fast inference. In *Advances in neural information processing systems*, pages 2946–2954, 2016.
- [12] Diederik Kingma and Jimmy Ba. Adam: A method for stochastic optimization. In *3rd International Conference on Learning Representations*, 2015.
- [13] Diederik Kingma and Max Welling. Auto-encoding variational Bayes. In *2nd International Conference on Learning Representations*, 2014.
- [14] Erich L Lehmann and George Casella. *Theory of point estimation*. Springer Science & Business Media, 2006.
- [15] Jure Leskovec and Andrej Krevl. SNAP Datasets: Stanford large network dataset collection. <http://snap.stanford.edu/data>, June 2014.
- [16] Yucen Luo, Tian Tian, Jiaxin Shi, Jun Zhu, and Bo Zhang. Semi-crowdsourced clustering with deep generative models. In *Advances in Neural Information Processing Systems*, pages 3212–3222, 2018.
- [17] Laurens van der Maaten and Geoffrey Hinton. Visualizing data using t-sne. *Journal of machine learning research*, 9(Nov):2579–2605, 2008.
- [18] Paolo Massa and Paolo Avesani. Trust-aware recommender systems. In *Proceedings of the 2007 ACM conference on Recommender systems*, pages 17–24. ACM, 2007.
- [19] Mathias Niepert, Mohamed Ahmed, and Konstantin Kutikov. Learning convolutional neural networks for graphs. In *International conference on machine learning*, pages 2014–2023, 2016.
- [20] Judea Pearl. Reverend bayes on inference engines: A distributed hierarchical approach. In *AAAI*, 1982.

- [21] Fabian Pedregosa, Gaël Varoquaux, Alexandre Gramfort, Vincent Michel, Bertrand Thirion, Olivier Grisel, Mathieu Blondel, Peter Prettenhofer, Ron Weiss, Vincent Dubourg, et al. Scikit-learn: Machine learning in python. *Journal of machine learning research*, 12(Oct):2825–2830, 2011.
- [22] Danilo Jimenez Rezende, Shakir Mohamed, and Daan Wierstra. Stochastic backpropagation and approximate inference in deep generative models. In *Proceedings of the 31st International Conference on Machine Learning*, pages 1278–1286, 2014.
- [23] Tianlin Shi, Da Tang, Liwen Xu, and Thomas Moscibroda. Correlated compressive sensing for networked data. In *Proceedings of the 30th Conference on Uncertainty in Artificial Intelligence*, pages 722–731, 2014.
- [24] Yoshio Takane, Forrest W Young, and Jan De Leeuw. Nonmetric individual differences multidimensional scaling: An alternating least squares method with optimal scaling features. *Psychometrika*, 42(1):7–67, 1977.
- [25] Da Tang and Tong Zhang. On the duality gap convergence of admm methods. *arXiv preprint arXiv:1508.03702*, 2015.
- [26] Da Tang, Dawen Liang, Tony Jebara, and Nicholas Ruoizzi. Correlated variational auto-encoders. In *International Conference on Machine Learning*, 2019.
- [27] Petar Veličković, William Fedus, William L Hamilton, Pietro Liò, Yoshua Bengio, and R Devon Hjelm. Deep graph infomax. In *7th International Conference on Learning Representations*, 2019.
- [28] Martin Wainwright and Michael Jordan. Graphical models, exponential families, and variational inference. *Foundations and Trends in Machine Learning*, 2008.
- [29] Martin J. Wainwright. *Stochastic processes on graphs with cycles: geometric and variational approaches*. PhD thesis, Massachusetts Institute of Technology, 2002.
- [30] Martin J Wainwright, Tommi S Jaakkola, and Alan S Willsky. A new class of upper bounds on the log partition function. *IEEE Transactions on Information Theory*, 51(7):2313–2335, 2005.
- [31] Pengcheng Yin, Chunting Zhou, Junxian He, and Graham Neubig. Structvae: Tree-structured latent variable models for semi-supervised semantic parsing. In *Proceedings of the 56th Annual Meeting of the Association for Computational Linguistics (Volume 1: Long Papers)*, pages 754–765, 2018.

Appendix

In the appendix, we provide more details on our baseline method CVAE [26] as well as the experiment data pre-processing and protocols.

A More details on CVAEs

CVAEs set the prior $p_0^{\text{corr}_g}(\mathbf{z})$ to be the uniform average over all of these tractable densities:

$$p_0^{\text{corr}_g}(\mathbf{z}) = \frac{1}{|\mathcal{A}_G|} \sum_{G'=(V,E') \in \mathcal{A}_G} p_0^{G'}(\mathbf{z}), \quad (12)$$

where $p_0^{G'}(\mathbf{z}) = \prod_{i=1}^n p_0(\mathbf{z}_i) \prod_{(v_i, v_j) \in E'} \frac{p_0(\mathbf{z}_i, \mathbf{z}_j)}{p_0(\mathbf{z}_i)p_0(\mathbf{z}_j)}$ is a prior on a maximal acyclic subgraph $G' = (V, E')$ with the same form as in Eq. 3. For each $G' \in \mathcal{A}_G$, we can similarly define a structured variational approximation $q_\lambda^{G'}(\mathbf{z}|\mathbf{x})$ following the form of Eq. 3:

$$q_\lambda^{G'}(\mathbf{z}|\mathbf{x}) = \prod_{i=1}^n q_\lambda(\mathbf{z}_i|\mathbf{x}_i) \prod_{(v_i, v_j) \in E'} \frac{q_\lambda(\mathbf{z}_i, \mathbf{z}_j|\mathbf{x}_i, \mathbf{x}_j)}{q_\lambda(\mathbf{z}_i|\mathbf{x}_i)q_\lambda(\mathbf{z}_j|\mathbf{x}_j)},$$

where $q_\lambda(\cdot|\cdot)$ and $q_\lambda(\cdot, \cdot|\cdot, \cdot)$ are two conditional density functions that captures the singleton and pairwise variational approximation densities. These two functions need to satisfy the symmetry and consistency properties:

$$\begin{cases} q_\lambda(\mathbf{z}_i, \mathbf{z}_j|\mathbf{x}_i, \mathbf{x}_j) = q_\lambda(\mathbf{z}_j, \mathbf{z}_i|\mathbf{x}_j, \mathbf{x}_i) & \text{for all } \mathbf{z}_i, \mathbf{z}_j, \mathbf{x}_i, \mathbf{x}_j, \\ \int q_\lambda(\mathbf{z}_i, \mathbf{z}_j|\mathbf{x}_i, \mathbf{x}_j) d\mathbf{z}_j = q_\lambda(\mathbf{z}_i|\mathbf{x}_i) & \text{for all } \mathbf{z}_i, \mathbf{x}_i, \mathbf{x}_j. \end{cases}$$

The ELBO in Eq. 5 is an average over potentially exponential many ELBOs. To make computations tractable, Tang et al. [26] simplifies this lower bound and represent it as

$$\begin{aligned} \mathcal{L}^{\text{CVAE}}(\lambda, \theta) := & \sum_{i=1}^n \left(\mathbb{E}_{q_\lambda(\mathbf{z}_i|\mathbf{x}_i)} [\log p_\theta(\mathbf{x}_i|\mathbf{z}_i)] - \text{KL}(q_\lambda(\mathbf{z}_i|\mathbf{x}_i)||p_0(\mathbf{z}_i)) \right) - \sum_{(v_i, v_j) \in E} w_{G, (v_i, v_j)}^{\text{MAS}} \\ & \cdot \left(\text{KL}(q_\lambda(\mathbf{z}_i, \mathbf{z}_j|\mathbf{x}_i, \mathbf{x}_j)||p_0(\mathbf{z}_i, \mathbf{z}_j)) - \text{KL}(q_\lambda(\mathbf{z}_i|\mathbf{x}_i)||p_0(\mathbf{z}_i)) - \text{KL}(q_\lambda(\mathbf{z}_j|\mathbf{x}_j)||p_0(\mathbf{z}_j)) \right). \end{aligned} \quad (13)$$

Where $w_{G, e}^{\text{MAS}} := \frac{|\{G' \in \mathcal{A}_G : e \in G'\}|}{|\mathcal{A}_G|}$ for each edge $e = (v_i, v_j)$ represents the fraction of G 's maximal acyclic subgraphs of G that contain e . These weights can be computed easily from the Moore-Penrose inverse of the Laplacian matrix of G .

B Experimental details

B.1 Dataset pre-processing details

Epinions We follow the same pre-processing scheme as Tang et al. [26]: binarize the rating data and create a bag-of-words binary feature vector for each user. We only retain the items that have been rated for at least 100 times. We construct the graph $G = (V, E)$ and only keep an edge (v_i, v_j) to be in E if both $v_i \rightarrow v_j$ and $v_j \rightarrow v_i$ appear in the original directed graph. At last, we only retain users that have at least one edge in E (i.e. having at least one bi-directional edge in the original dataset).

Citations This dataset includes the abstract and the citation information for high-energy physic theory papers on arXiv from 1992 to 2003. We work on all papers from 1998 in this dataset (in total $\approx 2.8\text{K}$ papers). We treat all citation edges as undirected edges and build the graph $G = (V, E)$. We only retain papers that cite or are cited by at least one of the other papers from the same year. We compute TF-IDF for the abstract of each paper as feature vector.

B.2 Experimental protocol

We run 3 runs for each methods for the Epinions experiment and 5 runs for each methods for the Citations experiment, as the Epinions experiments work more stable empirically.

For VAE, CVAE and ACVAE, we apply a two-layer feed-forward neural inference network for the singleton variational distribution $q_{\lambda}(z_i|x_i)$'s and a two-layer feed-forward neural generative network for the model distribution $p_{\theta}(x|z)$'s. $q_{\lambda}(z_i|x_i)$ is a diagonal normal distribution with the mean and standard deviation outputted from the inference network and $p_{\theta}(x|z)$ is a multinomial distribution with the logits outputted from the generative networks. The latent dimensionality d is 100 for the Epinions dataset and 10 for the Citations dataset. The hidden layer dimensionality h_1 is 300 for the Epinions dataset and 30 for the Citations dataset.

For GraphSAGE, we choose to use $K = 2$ aggregation, the mean aggregator, and $Q = 20$ negative samples to optimize the loss function. The hidden layer size and latent dimensionality we apply to GraphSAGE are the same with that of the standard VAE.

For CVAE and ACVAE, we set the pairwise marginal prior density function to be $p_0(\cdot) = \mathcal{N}\left(\mu = \mathbf{0}_{2d}, \Sigma = \begin{pmatrix} I_d & \tau \cdot I_d \\ \tau \cdot I_d & I_d \end{pmatrix}\right)$ with $\tau = 0.99$. For CVAE_{corr} and ACVAE, we model the pairwise variational approximations $q(z_i, z_j|x_i, x_j)$ to be a multi-variate normal distribution that can be factorized across the d dimensions as the product of d independent bi-variate normal distributions. The correlation coefficients of these bi-variate normal distributions are computed from two-layer feed-forward neural networks that taking x_i and x_j as inputs. These two-layer neural networks have latent dimensionality h_2 to be 1000 for the Epinions experiment and 30 for the Citations experiment. For CVAE and ACVAE, we set the negative sampling parameter γ to be 1000 for the Epinions experiment and 100 for the Citations experiment. This parameter is selected from $\{0.1, 1, 10, 100, 1000\}$ and select the values based on performances.

For all methods, we look into the performances for every fixed number of iterations (the specific numbers depend on models) and update the current best test NCRR values if both the train objective and the train NCRR reach better values. We report the final current best test NCRR values as the results.

For ACVAE, we set the step size parameter (in Eq. 10) $\alpha^t = 0.1$ to be a constant. We train the parameters using alternating updates as in Algorithm 1. We switch between updates on the parameters λ, θ for an epoch of the edges in E , and a single update on the weights $w_{G,\pi,e}^{\text{MAS}}$ according to Eq. 10. For the random initialization on the tree weights $w_{G,\pi,e}^{\text{MAS}}$, we just assign random weights to the graph $G = (V, E)$. Then we use Kruskal's algorithm to compute the maximal acyclic subgraph $\tilde{G} = (V, \tilde{E})$ according to these random weights, and set $w_{G,\pi,e}^{\text{MAS}} = I[e \in \tilde{E}]$. It is straightforward to see that this is a valid initialization for the weights $w_{G,\pi,e}^{\text{MAS}}$'s since these weights relate to the distribution $\tilde{\pi}$ that has all of its mass on the single subgraph \tilde{G} .

For all methods, we apply stochastic gradient optimizations and use Adam [12] to adjust the learning rates. We set the step size to be 10^{-3} . For all methods, we use a batch size $B_1 = 64$ for sampling the vertices. For CVAE and ACVAE, we use a batch size $B_2 = 256$ for sampling the edges and non-edges.

All experiments are done using Python. The training and evaluations are done with TensorFlow [1] and Numpy. The TF-IDF values and the t-SNE embeddings [17] in the visualization (Figure 1(b)) are computed using Scikit-learn [21]. For faster computations, we call C++ functions to do belief propagation and the Kruskal's algorithm using Cython [2].